



OPEN Gestational high-sucrose diet mediated vascular hypercontractility in mesenteric arteries from offspring

Xinying Liu^{1,4}, Meng Liu^{2,4}, Chunxia Wang¹, Liting Duan¹, Qinggui Ren³, Shuli Jiang¹, Jing Han¹, Hongwei Fu², Xiao Sun², Dongmei Man¹✉ & Xueqin Feng¹✉

Prenatal high sucrose diet (HS) generates profound effects on vascular diseases in offspring later in life. This study aimed to determine whether and how prenatal HS affect vasoreactivity in resistance arteries from adult offspring. Pregnant Sprague-Dawley rats were fed with normal drinking water or 20% high-sucrose solution during the whole gestational period. Mesenteric arteries (MAs) from adult offspring were obtained and tested for vascular functions with DMT. The whole-transcriptome sequencing (RNA-seq) of MAs was performed to reveal the different genes and possible pathway. Real-time PCR and western blot were performed to access mRNA and protein expression. The thicker smooth muscle layer and mitochondrial swelling were observed in MAs in HS offspring. Prenatal HS mediated higher vasoconstriction/vascular sensitivity induced by phenylephrine (PE) and 5-Hydroxytryptamine (5-HT). RNA-Seq analysis revealed that the genes crystallin alpha B (CYRAB) and heat shock protein family E member 1 (HSPE1) were upregulated, while the gene adenomatous polyposis coli downregulated 1 (APCDD1) was downregulated in HS group, confirmed at mRNA and protein expression levels. Wntless-related integration site (Wnt)/Ca²⁺ indicated by KEGG analysis was the essential pathway inducing vascular dysfunction in HS group. As a Wnt5a inhibitor, Box5 reduced MA tension induced by PE or 5-HT in HS group. Both protein kinase C (PKC) inhibitor-GF109203X and Inositol 1,4,5-trisphosphate receptor (IP3R) inhibitor-2-Aminoethoxydiphenyl borate (2-APB) significantly decreased MA tone in HS group. Ca²⁺ levels in MAs were markedly higher in HS offspring than in control (CON), likely contributing to enhanced vascular reactivity. Vascular relaxation induced by acetylcholine (ACh) in HS was lower than that in CON. N(G)-Nitro-L-arginine methyl ester (L-NAME) increased PE-mediated vascular tension in CON group, while no effect in HS group, suggesting that endothelial nitric oxide (NO) system dysfunction in MAs exposed to prenatal HS. This study demonstrated that prenatal HS induced hyper-vasocontraction in MAs from adult offspring, which was associated with the enhanced Wnt5a-PKC/IP3R-Ca²⁺ pathway and decreased endothelial NO function.

Keywords Prenatal high-sucrose, Mesenteric artery, Vasoconstriction, Wnt, NO

Epidemiological evidence establishes a dose-dependent relationship between chronic high-sucrose diets and cardiometabolic risk¹. The NHANES cohort demonstrates that individuals exceeding 15% daily energy intake from sucrose exhibit a 2.3-fold elevated incidence of hypertension, with heightened vulnerability observed in populations exposed during developmental windows². Maternal nutritional perturbations during gestation induce persistent cardiovascular reprogramming in offspring, as evidenced by vascular dysfunction in prenatal high-sucrose exposure model³. Notably, this developmental programming may involve Wnt signaling cascades, though the precise molecular architecture remains undefined.

In the vascular system, Wnt signaling has been shown to be involved in vascular development, angiogenesis, and vascular remodeling⁴. As an important member, the Wnt/Ca²⁺ pathway is predominantly activated by the Wnt5a ligand and Fzd2 receptor, and plays an important role in vascular contraction⁵. Mechanistically, Wnt5a, as a crucial ligand within the non-canonical Wnt signaling pathway⁶, is activated upon binding to the corresponding

¹Department of Obstetrics, Affiliated Hospital of Jining Medical University, 272001 Jining, China. ²Department of Clinical Medicine, Jining Medical University, 272067 Jining, China. ³Department of Mammary Gland Surgery, Affiliated Hospital of Jining Medical University, 272001 Jining, China. ⁴Xinying Liu and Meng Liu have contributed equally to this work. ✉email: mandongmei@163.com; fengxueqin4443@126.com

receptors located on the surface of vascular cells. Upon activation, the signaling cascade initiates the activation of protein kinase C (PKC). Subsequently, the activated PKC exerts its action on inositol trisphosphate receptors (IP3R)⁷. IP3Rs are accountable for regulating the release of intracellular calcium ions. The dynamic alterations in Ca²⁺ concentration directly impact the contraction and relaxation of vascular smooth muscle, thereby regulating vascular tone and blood pressure⁴. Furthermore, this pathway is implicated in the regulation of vascular endothelial-cell functions, exerting an impact on vascular homeostasis and repair processes. In summary, the Wnt5a-PKC/IP3R-Ca²⁺ pathway is of paramount importance for maintaining normal vascular functions.

As pivotal regulators of peripheral resistance, mesenteric arteries are abundant in vascular smooth muscle cells and have small lumen diameter. Third-order mesenteric arteries contribute 35% to systemic blood pressure control through dynamic tone modulation⁸. Their vascular smooth muscle cells exhibit a distinct receptor profile, including enriched Frizzled-2 (Fzd2) expression and PKC/IP3R colocalization, making them an optimal model for studying non-canonical Wnt signaling. Therefore, it is essential to investigate the effect of prenatal high-sucrose diet on mesenteric arteries from adult offspring. Addressing such questions is crucial to further understanding vascular diseases of developmental origins.

This study postulates the hypothesis that antenatal high-sucrose exposure programs offspring vascular dysfunction through Wnt5a-mediated activation of the PKC/IP3R signaling axis to trigger alterations in calcium ion levels. These changes in Ca²⁺ levels further increase the likelihood of the onset of cardiovascular diseases. Given the protective effect of estrogen in the cardiovascular system of females, only male offspring were separated and used for further study. If this hypothesis holds true, it will reveal a novel mechanism by which prenatal high-sucrose exposure impacts the cardiovascular health of offspring and offer a theoretical basis for the early prevention and intervention of related diseases.

Materials and methods

Animals

The study was conducted in accordance with the Animal Research: Reporting of In Vivo Experiment (ARRIVE) guidelines. All experiments were approved by the Ethical Committee of the Affiliated Hospital of Jining Medical University (No: 2020B010) and in accordance with the Care and Use of Laboratory Animals (NIH Publication No. 85–23, 1996).

Sprague–Dawley rats (3-month old male: 350–400 g, female: 240–270 g) were purchased from Peng Yue Experimental Animal Breeding Company. They were housed in a controlled environment of 25 °C under a 12 light–dark cycle with cycles of air ventilation, free access to water and standard food. After 1 week of recovery of transportation, female rat was mated with male rat. The day vaginal plugs were detected was regarded as the first day of gestation. Total pregnant rats were randomly assigned to two groups: the high-sucrose group (HS) was fed with the standard food and 20% sucrose solution (20% sucrose dissolved in drinking water), and the control group (CON) was provided with standard food and tap water from gestational day 1 to day 20. All pregnant rats ($N=20$ each group) were allowed to give birth naturally. After being anesthetized with sodium pentobarbital (50 mg/kg), the male offspring were sacrificed at 4 months old to isolate mesenteric artery (MA) for experiments and the offspring did not receive any treatment during the study. In the study, 4-month-old Sprague–Dawley rats were utilized to model human young adulthood, corresponding to the post-pubertal stabilization phase in rodents without age-related metabolic decline. Metabolomic analyses confirm that insulin sensitivity and lipid turnover rates in 4-month-old rats demonstrate strong comparability with human young adult population^{9,10}. For all experiments, including molecular analyses, the pups used were from different litters each group.

Hematoxylin and eosin (HE) staining

Mesenteric arteries from adult offspring were isolated and immediately fixed in 4% paraformaldehyde, embedded in paraffin, and sectioned at 5 μ m in thickness. The paraffin-embedded sections were dehydrated using xylene and graded ethanol. Then, the sections were stained with hematoxylin solution and eosin-phloxlike B solution. After washing with distilled water, samples were analyzed by Olympus BX53 biological microscope. The vessel wall thickness was measured with calibrating the software and analyzed with Image J 1.x (Bethesda, MD, USA) and GraphPad Prism 9.4 (GraphPad, San Diego, California, USA).

Transmission electron microscopy

The MAs from adult offspring were fixed in 2.5% glutaraldehyde (pH = 7.4) for 2 h. After washed three times with 0.1 M phosphate buffer (pH = 7.2), the vessels were fixed again in 1% osmic acid at 4 °C for 2 h. Then the samples were gradient dehydrated with ascending concentrations of ethanol. Subsequently, the MAs were subjected to resin penetration and embedded in epon. After position, the ultrathin section was made and counterstained with 3% uranyl acetate and 2.7% lead citrate. Finally, the sections were observed with a HT7800 transmission electron microscope.

Measurement of vascular tension

Mesenteric arteries were cut into 2.0 mm in length and recorded with multi-myograph system (Danish Myo Technology, Denmark). The organ chamber was filled with 5 mL PSS solution (mmol/L: NaCl, 120.9; NaHCO₃, 25.0; KCl, 4.7; MgSO₄·7H₂O, 1.7; CaCl₂·2H₂O, 2.8; EDTA, 0.025; KH₂PO₄, 1.2; and glucose, 5.0; 4 °C, pH = 7.4), continuously gassed with 95% O₂–5% CO₂. Each vessel ring was tested only once in this study. KCL (120 mmol/L)-mediated vascular contraction was regarded as contraction normalization. After equilibration for 30 min, cumulative doses (10^{−9} to 10^{−4} mol/L) of phenylephrine (PE) or serotonin (5-HT) was used to test vascular tension, while acetylcholine (ACh) also used to assay vasodilatory. The effect of endothelial nitric oxide synthase (eNOS) was analyzed by preincubating vascular segments with NG-nitro-L-arginine (L-NAME, eNOS inhibitor, 10^{−4} mol/L) before doses of PE/5-HT were added. To detect whether the Wnt5a/Ca²⁺ signals cause

abnormal vasoconstriction, Box5 (antagonist for Wnt5a, 10^{-5} mol/L), 2-APB (antagonist for IP3R, 10^{-5} mol/L), or GF109203X (antagonist for PKC, 10^{-6} mol/L) was used for pretreating segments for 30 min respectively before application of PE or 5-HT. Signals were recorded with Power-Lab system with Chart 7.0 software (AD Instruments, USA) for analysis.

RNA-sequence (RNA-Seq)

The RNA-Seq was performed with assistance from Shandong Jieluoxuan Biotechnology co.,ltd (Shandong, China). Magnetic beads with Oligo (dT) were used for RNA enrichment and purification. The rRNA was removed by kit as instruction described (Agilent Technologies, CA, USA). In brief, fragmentation buffer was added into the purified mRNA to shorten the fragments. The first strand of cDNA was synthesized by using random primers. The 2nd strand marking buffer and 2nd strand/end repair enzyme mix were added to synthesize the 2nd strand of cDNA. Following the terminal repair, base A and sequencing joint were added. Sequentially, the target fragment was recovered by magnetic bead screening, and PCR amplification was performed to complete the whole library preparation. After the library was constructed, Qubit 3.0 was used for initial quantification and the library was diluted to 1 ng/ul, followed by Agilent 2100. Once the insert size met expectation, Q-PCR was performed using Bio-Rad CFX 96 fluorescence quantitative PCR instrument and Bio-Rad kit iQ SYBR GRN. The effective concentration of the library was quantified accurately (effective concentration > 10 nM) to ensure the quality. Qualified library was sequenced on a high-throughput sequencing platform.

Real-time PCR

Total RNA of MAs was extracted using RNA-easy Isolation Reagent (Vazyme, USA) following the manufacturer's instructions. The RNA concentration and purity were confirmed by spectrophotometer (Thermo, USA). First-strand cDNA was synthesized by HiScript III RT SuperMix. Real-time PCR was performed in 20 μ L system including 10 μ L of ChamQ Universal SYBR RT-RCR Master Mix, 0.4 μ L of forward primer (10 μ M), 0.4 μ L of reverse primer (10 μ M), 2 μ L cDNA, and 7.2 μ L of nuclease-free water, and was carried out using MyiQ2 Thermal Cycler Real-Time PCR Detection System (Bio-Rad, USA) according to the following program: one cycle at 95 $^{\circ}$ C for 30 s; 40 cycles of 10 s at 95 $^{\circ}$ C, and 30 s at 60 $^{\circ}$ C; one cycle at 95 $^{\circ}$ C for 15 s, 60 $^{\circ}$ C for 60 s and 95 $^{\circ}$ C for 15 s. Expressions of genes were normalized to β -actin. The gene primer sequences were shown in Table 1.

Western blot

The MAs were homogenized in liquid nitrogen and lysed in RIPA buffer (Beyotime Biotech, China) containing protease inhibitors and phosphatase inhibitors (Biotool, China) to obtain the whole cell protein. Samples with equal total proteins were separated by 10% polyacrylamide gel and transferred onto polyvinylidene fluoride membranes. Following blocking non-specific binding sites by 5% skim milk, the PVDF membranes were incubated with the primary antibodies, including GAPDH (1:2000, Affinity, China), β -actin (1:5000, Affinity, China), Wnt5a (1:1000, Affinity, China), PKC α (1:1000, Abcam, US), CRYAB (1:1000, Absin, China), HSPE1 (1:1000, Absin, China), and APCDD1 (1:1000, Proteintech, China). Following removal of the primary antibody, it was incubated with HRP-coupled goat anti-rabbit secondary antibody (1:5000, Proteintech, China) for 1 h on a shaker at room temperature. Blots were visualized using enhanced chemiluminescence detection reagents (Thermo Fisher, Australia), and were recorded using an Imaging System (Tanon, Shanghai, China). Specific bands were quantified using Image J 1.x (Bethesda, MD, USA).

Elisa

The levels of Ca²⁺ and O₂⁻ in mesenteric artery tissues were measured by commercialized Calcium Assay Kit (JL-T0845, JONLNBIO, China) and Superoxide Anion Assay Kit (JL-T0783, JONLNBIO, China), respectively. For Ca²⁺ determination, in an alkaline solution, Ca²⁺ form a purple-red complex with O-cresolphthalein complexone (OCPC) in the presence of a magnesium ion chelator, which mitigates background interference from magnesium ions. The absorbance of this complex is measured at 575 nm with microplate reader. Regarding O₂⁻ measurement, O₂⁻ react with hydroxylamine to generate nitrite (NO₂⁻), which, in the presence of sulfanilic acid and α -naphthylamine, forms a pink azo dye. The absorbance of this dye is measured at 540 nm with Synergy H1 microplate reader (BioTek Instruments, USA). Ca²⁺ concentration and the O₂⁻ concentration are calculated based on a standard curve, respectively.

| Gene | Forward primer (5'-3') | Reverse primer (3'-5') |
|----------------|------------------------|--------------------------|
| APCDD1 | TGAGACCGAGAGAGCATCCA | TCTACACCGCAACCCAGAAC |
| Wnt5a | TCTTCAGCCATTCACACCAT | CAGAGAAGGGAGGCTCACC |
| IP3R | AGCAGCAGCAGCAGCAGCAG | CTGCTGCTGCTGCTGCTGCT |
| PKC α | GAGCAGGAGAGCGTGAAAGA | TCCTTGTGCTTCACGAGCAT |
| PKC δ | CGCAGATGATCTCAGCTGC | CCATCTCATCTGTACCTTCCAGAC |
| PKC ϵ | CCATCAGAAGACGACCGATC | CCATCAGTAGACGACGAGGCT |
| β -actin | CCGCCCTAGGCACCGGGTG | GGCTGGGGTGTGAAGGTCTCAAA |

Table 1. Primer sequences used in the study.

Statistical analysis

Figure 1 showed the flow diagram of our study. All experimental data were presented as mean \pm SEM, and analyzed with unpaired t-test or two-way ANOVA followed by Bonferroni, where appropriate. The data were performed and curve fitted with GraphPad Prism 9.4 (GraphPad, San Diego, California, USA), Image J 1.x (Bethesda, MD, USA) and LabChart Version 7.0. (AD Instruments Pty Ltd. Shanghai, China). Statistical significance was defined as $p < 0.05$. N represents the number of pregnancy and n represents the offspring number from different litters.

Results

HE stains and transmission electron microscopy (TEM)

Vascular gross morphology of the MAs from CON and HS groups was assessed with HE stains. The vascular wall of the smooth muscle layer thickness in HS group was thicker than that in CON group (Fig. 2A). The microstructure of MAs was further observed by TEM. Compared with the CON group, we found the mitochondrial injury with the higher mitochondrial area in the HS offspring characterized by mitochondrial swelling in vascular smooth muscle cells of MAs (Fig. 2B). It suggested that prenatal HS altered the vascular structure of MAs in offspring.

Given the well-established link between mitochondrial function and oxidative stress, and considering the observed mitochondrial injury in the HS group, we hypothesized that there might be an associated change in oxidative stress balance. Impaired mitochondrial function may lead to an abnormal production of O_2^- . As expected, the levels of O_2^- were significantly increased in the HS group compared to the CON group (Fig. 2C). The series of results thus not only revealed the structural changes in the vasculature but also elucidated the underlying oxidative stress-related mechanisms triggered by prenatal HS.

The effect of prenatal HS on vascular contractions of MAs from offspring

Vascular function was further determined with DMT. There was no significant difference in KCL-induced max vasoconstrictions between the two groups (Fig. 3A). Both PE and 5-HT produced dose-dependent contraction in MAs (Fig. 3B, C). However, concentration response curve of PE/5-HT-induced vascular tension and pD2 (-logEC50) in HS group were significantly greater than that in the CON group (Fig. 3B, E). The data suggested that prenatal HS increased vascular tension and contraction sensitivity.

RNA-Seq analyses

To further clarify the underlying mechanism of vascular function changed in HS group, the MAs were collected for RNA-Seq. Three significant expressed genes were selected in HS group, including downregulation of APCDD1 and upregulation of CRYAB and HSPE1 (Fig. 4A, B), and confirmed by mRNA and protein detection (Fig. 4C, D). In addition, KEGG pathway enrichment analyses^{11–13} indicated that protein-binding, ion-binding, and Wnt-protein pathway have higher enrichment score (Fig. 4E).

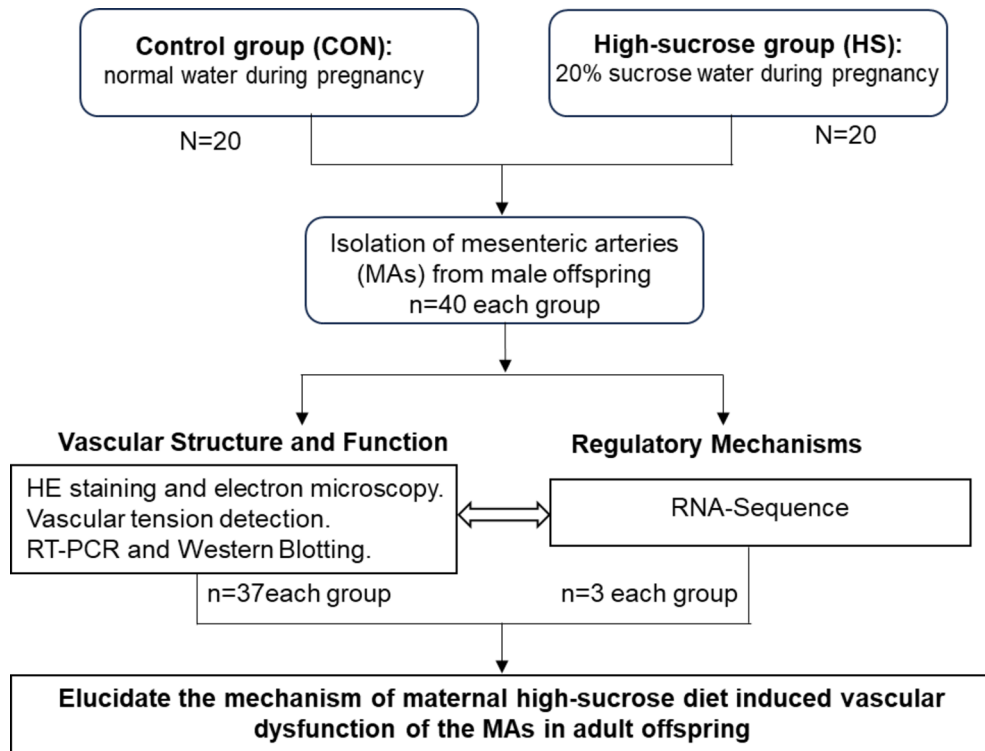


Fig. 1. Experimental design and workflow.

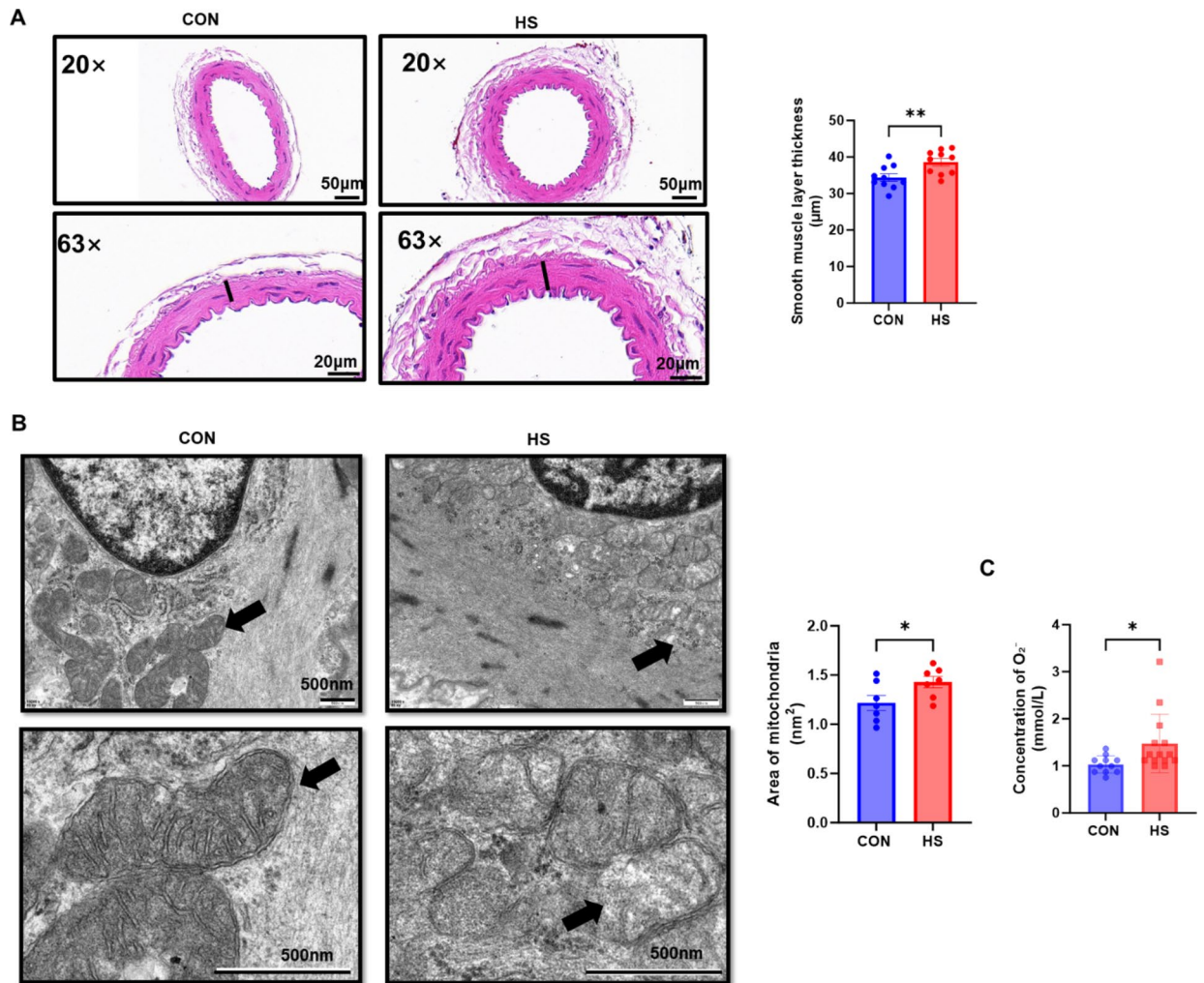


Fig. 2. HE staining and transmission electron microscopy of MAs from offspring. **(A)** HE staining of MAs. Bar: 50 µm (20×), 20 µm (63×). **(B)** Transmission electron microscopy of MAs. **(C)** The concentration of superoxide anions (O_2^-) in MAs. Bar: 500 nm. Arrow indication: mitochondria. Black line is utilized to denote the measured thickness of the smooth muscle layer. $n = 7-14$ from different litters. * $p < 0.05$, ** $p < 0.01$.

The role of Wnt5a/ Ca^{2+} signaling pathway in MAs dysfunction in HS

We employed the Wnt5a inhibitor, Box5, to assay the vascular tension. As Fig. 5A, B showed Box5 could notably decrease PE or 5-HT-mediated vascular constriction in HS group. The mRNA and protein expressions of Wnt5a were significantly elevated in HS group (Fig. 5C). The data revealed that vascular hyper-contractility in HS was resulted from hyperactive Wnt5a signaling pathway. We then investigated how Wnt5a signaling pathways participated in the vascular regulation in MAs in HS. As shown in Fig. 5D, E, GF109203X, PKC inhibitor, could notably decrease the higher vascular tension induced by PE or 5-HT in HS group, suggesting that PKC signal was involved in regulating vascular dysfunction in HS, further confirmed by the mRNA and protein expressions (Fig. 5F). 2-APB, the IP3R antagonist, also reduced the increased vascular tone induced by PE or 5-HT in HS group (Fig. 5G, H), and the mRNA expression of IP3R was also up-expressed in MAs exposed to prenatal HS (Fig. 5I). Meanwhile, the concentration of Ca^{2+} was significantly higher in HS group (Fig. 5J), as determined by statistical analysis. The above data strongly suggested that prenatal HS induced vascular dysfunction via activating Wnt5a-PKC/IP3R- Ca^{2+} pathway.

Endothelial NO synthase in MAs dysfunction in HS

Besides the clues indicated by RNA-Seq, Wnt5a could also regulates vascular function via controlling endothelial cells. Therefore, we further detected endothelial function with ACh, a drug that mediates endothelium-dependent vasodilation. In both the CON and HS groups, ACh produced dose-dependent dilations following PE-induced contraction platform, and ACh-induced dilation in HS group was weaker than that in the CON group (Fig. 6A). In addition, the role of eNOS in the vascular tension was further determined by employing eNOS inhibitor, L-NAME. As Fig. 6B showed that L-NAME notably increased PE-mediated constriction significantly in the CON but not the HS group. The above data indicated that prenatal HS also induced endothelial dysfunction in MAs from adult offspring.

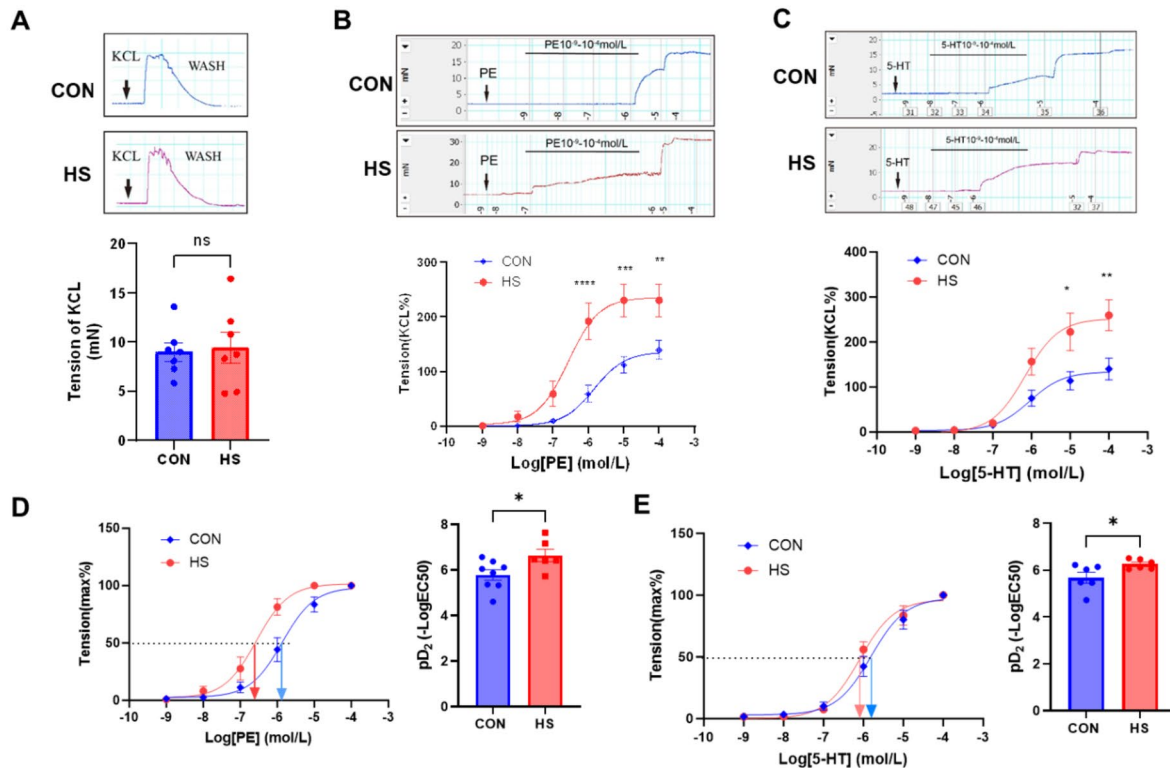


Fig. 3. The effect of prenatal HS on vascular tension of MAs from offspring. **A** KCL-mediated contraction in MAs. **B** PE-mediated contraction in MAs. **C** 5-HT-mediated contraction in MAs. **D** PE-mediated contraction sensitivity expressed as pD_2 ($-\text{LogEC}_{50}$) in MAs. **E** 5-HT-mediated contraction sensitivity expressed as pD_2 ($-\text{LogEC}_{50}$) in MAs. $n = 7-10$ from different litters. * $p < 0.05$, ** $p < 0.01$, *** $p < 0.001$, **** $p < 0.0001$.

Discussion

Abnormal vascular development might increase morbidity of cardiovascular diseases¹⁴. In the study, we examined the hypothesis that antenatal HS exposure mediated vascular dysfunction through activating Wnt5a-PKC/IP3R- Ca^{2+} signaling pathway and inducing endothelial NO system dysfunction in MAs offspring. The main results in the study were as follows: (1) prenatal HS elevated PE/5-HT-induced vasoconstriction in the MAs in adult offspring. (2) RNA-seq analysis indicated that HSPE1 and CRYAB may participate in the regulation of vascular dysfunction via Wnt5a-PKC/IP3R- Ca^{2+} signaling in MAs in HS group. (3) prenatal HS induced endothelial NO system dysfunction in MAs from adult offspring. Figure 7 summarized the working model.

Previous studies have established that adverse dietary patterns during pregnancy could impose detrimental impacts on the metabolic and cardiovascular systems of offspring¹⁵. Consistent with our findings, offspring exhibit vascular dysfunction in adulthood. Abnormal vascular contractility may lead to hypertension, atherosclerosis, and other cardiovascular diseases in the later life^{16,17}.

Vascular functions fundamentally rely on the structure, ranging from the macroscopic tissue composition of vessel walls to the microscopic morphology of mitochondria¹⁶. As indicated, vascular thickness and mitochondrial morphology were altered in MAs exposed to prenatal HS, suggesting that prenatal HS exposure affected vascular structure in offspring. Maternal HS diet during pregnancy may promote the proliferation of vascular smooth muscle cells, leading to thickening of the vascular muscle layer in offspring. Mitochondria, the key cellular organelles, link the morphological integrity to functions such as energy metabolism and cell signaling, thereby influencing vascular activities including constriction, dilation, and material transport⁷. Altered mitochondrial morphology can impair ATP synthesis, increase O_2^- generation, and disrupt calcium balance¹⁸. These changes cascade through cellular functions, particularly vascular smooth muscle cells. In our study, the increased O_2^- concentration in the MAs of the HS offspring reflected the alteration of the oxidative stress balance, which may influence MAs functions in HS offspring, serving as one of the key factors contributing to the pathogenesis of cardiovascular diseases, as consistently evidenced by another study¹⁹.

As assumed, vasoconstriction and drug sensitivity were notably increased in MAs exposed to prenatal HS. To explore the specific mechanisms underlying vascular dysfunction in HS, RNA-Seq of MAs was performed. The RNA-Seq results indicated that Wnt/ Ca^{2+} signal may participate in MAs function regulation in HS. Ca^{2+} linked closely with the development of various cardiovascular diseases²⁰. For instance, Ca^{2+} overload can enhance the contractile function of cardiomyocytes, leading to myocardial hypertrophy and heart failure²¹. To date, Wnt5a is the best-studied non-canonical Wnt ligand in cardiovascular diseases²². By applying the Wnt5a inhibitor-

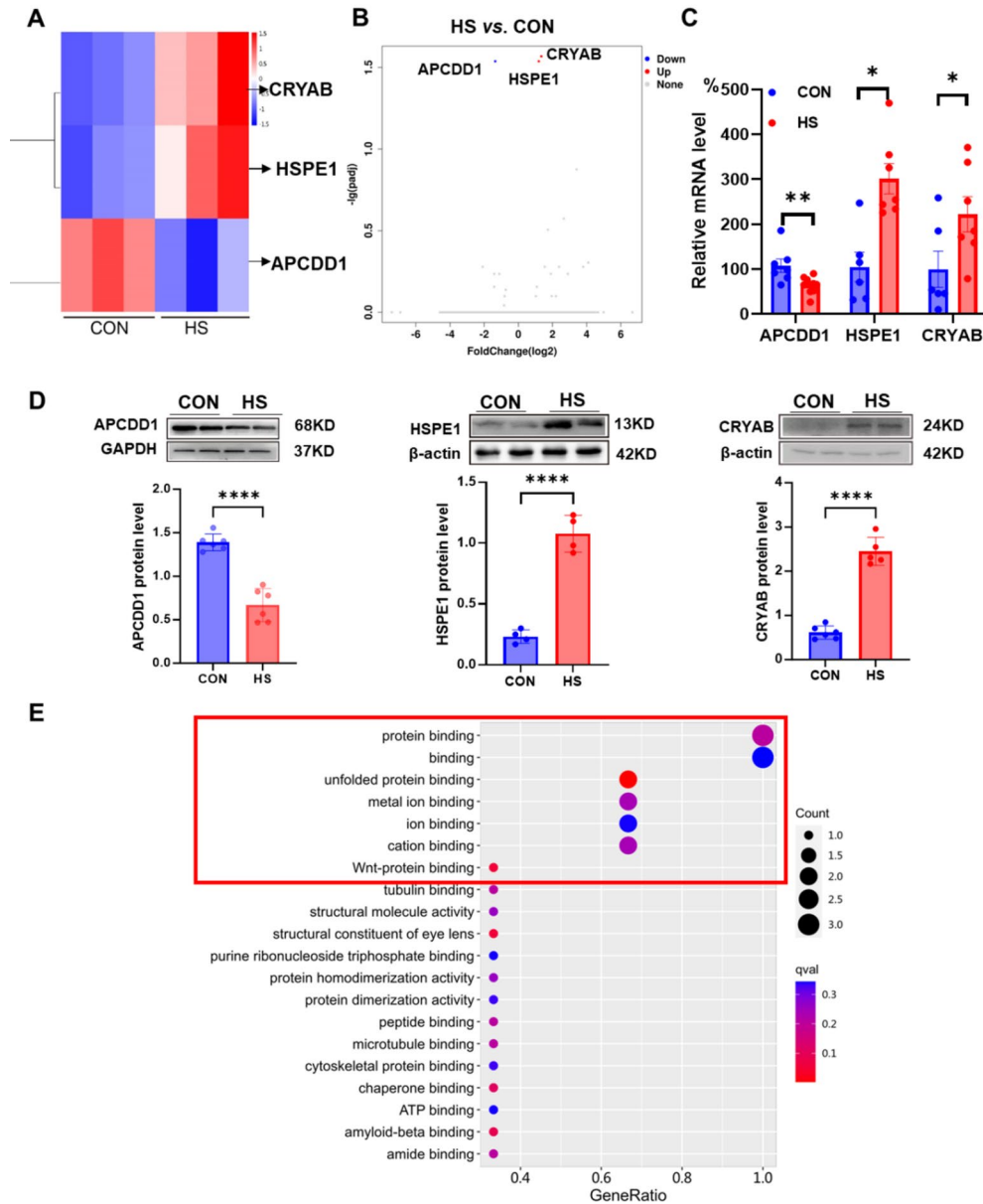


Fig. 4. The RNA-Seq analysis of MAs from offspring. **A** Heat map of RNA-Seq. CON: $n = 3$, HS: $n = 3$. **B** Volcano map of RNA-Seq. CON: $n = 3$, HS: $n = 3$. **C** The mRNA expressions of APCDD1, HSPE1 and CRYAB. **D** The protein expressions of APCDD1, HSPE1 and CRYAB. **E** KEGG pathway enrichment analyses. $n = 3-7$ from different litters. * $p < 0.05$, ** $p < 0.001$, **** $p < 0.0001$.

Box5 in MAs, it was further confirmed that Wnt5a/ Ca^{2+} was involved in the MAs dysfunction in HS group. To the best of our knowledge, it was the first demonstration that prenatal HS influenced the function of the non-canonical Wnt signal pathway in MAs. Wnt5a could further activate PKC and IP3R by triggering Fzd2/PLC/PIP²³. Under high-glucose conditions, both the activity and tissue distribution of PKC isoforms were enhanced²⁴. PKC α , PKC δ and PKC ϵ were detected in the rat mesenteric arteries. PKC α , high expression within MAs in HS, could increase intracellular Ca^{2+} via phosphorylation calcium channel²⁵. By applying GF109203X, the functional experiment detected by DMT further validated that PKC was involved in the MAs regulation in HS. The Ca^{2+} releases from the sarcoendoplasmic reticulum depends on IP3R²⁶. In the present study, the activities of IP3R were upregulated in HS group, similar to the findings in previously published research of thoracic aortic vessels with hypoxic models²⁰. This congruence not only validates the current research but also implies that the underlying mechanisms related to IP3Rs regulation might be conserved across different physiological stress models and vascular tissues. It further provides a broader context for understanding the role of IP3Rs in mediating the effects of prenatal insults on vascular function, which could potentially contribute to

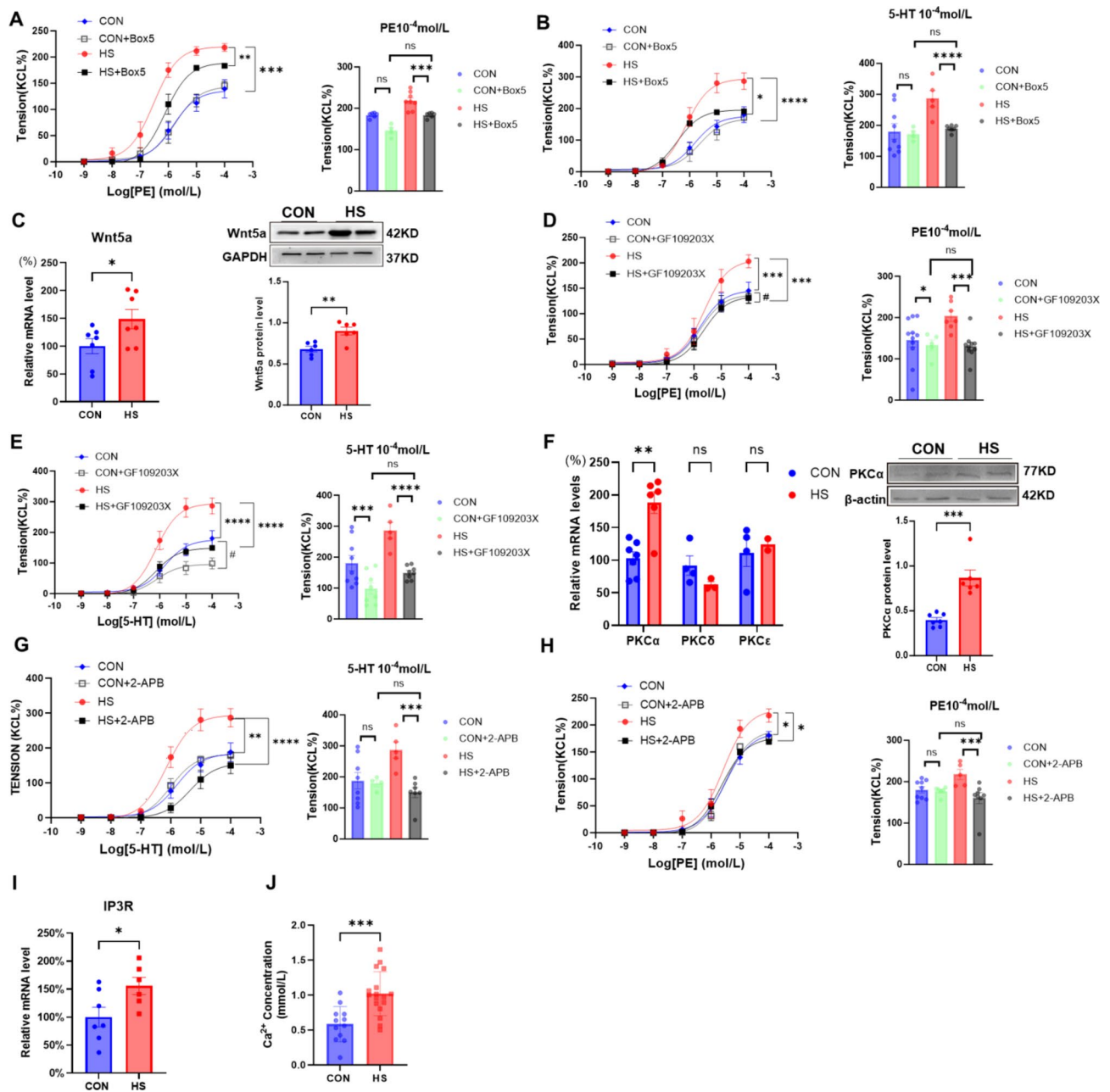


Fig. 5. Wnt5a-PKC/IP3R-Ca²⁺ signaling in MAs from offspring exposure to prenatal HS. **A** PE-induced contraction with or without Box5 (Wnt5a inhibitor). **B** 5-HT-induced contraction with or without Box5 (Wnt5a inhibitor). **C** The mRNA and protein expression of Wnt5a. **D** PE-induced contraction with or without GF109203X (PKC inhibitor). **E** 5-HT-induced contraction with or without GF109203X (PKC inhibitor). **F** The mRNA levels of PKC α , PKC δ , and PKC ϵ , and protein expression of PKC α . **G** PE-induced contraction with or without 2-APB (IP3R inhibitor). **H** 5-HT-induced contraction with or without 2-APB (IP3R inhibitor). **I** The mRNA level of IP3R. **J** Ca²⁺ concentration in MAs. *n* = 5–14 from different litters. #, **p* < 0.05, ***p* < 0.01, ****p* < 0.001, *****p* < 0.0001.

the development of more targeted preventive and therapeutic strategies for related cardiovascular disorders in offspring exposed to prenatal high-sucrose insults.

Besides vascular smooth muscle cells, endothelium is another important factor to regulate vascular function. The activation of aberrant Wnt signaling could induce abnormal vascular development by initiating the process of endothelial dysfunction²². Ca²⁺ plays a significant role in regulating endothelial cell function. Elevated levels of Ca²⁺ can lead to endothelial dysfunction, characterized by reduced endothelium-dependent vasodilation, thereby affecting the normal physiological functions of blood vessels. To determine whether the endothelial function was altered in MAs from the HS group, ACh and L-NAME were used to detect endothelium-dependent relaxation in MAs²⁷. ACh causes vascular relaxation by stimulating the endothelium to produce NO, and our

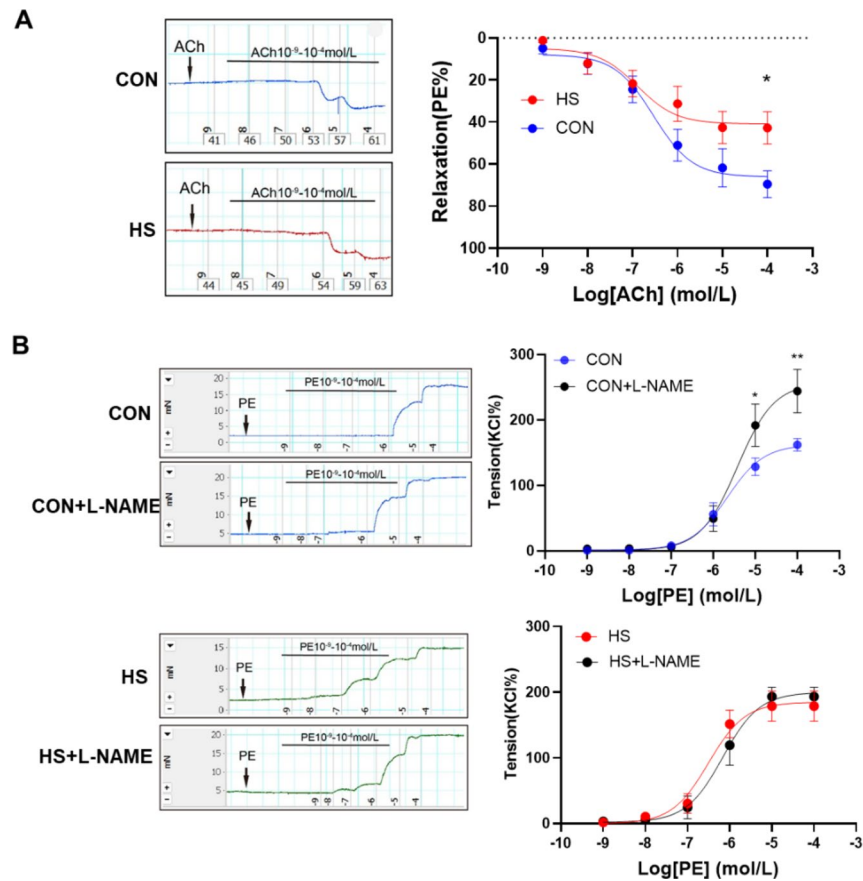


Fig. 6. The effect of prenatal HS on endothelial NO function in MAs from offspring. **A** ACh-induced vasodilatation following PE-mediated contraction in the MAs. **B** PE-induced contraction with or without L-NAME. $n = 4-6$ from different litters. * $p < 0.05$, ** $p < 0.01$.

data showed that ACh-induced relaxation was significantly decreased in HS. In addition, L-NAME significantly potentiated PE-mediated vasoconstrictions in the CON group, while no difference was found in HS. These data indicated that the endothelium NO system dysfunction might further contribute to vascular hyper-vasoconstriction in MAs exposed to prenatal HS.

In conclusion, prenatal HS induced vascular hyper-contraction in MAs from the adult offspring, which was result from the enhanced Wnt5a-PKC/IP3R-Ca²⁺ pathway in vascular smooth muscle and the decreased endothelial NO function, offering new information for understanding and therapeutic targeting vascular dysfunction in offspring exposed to prenatal nutrition, especially prenatal high-sucrose diet.

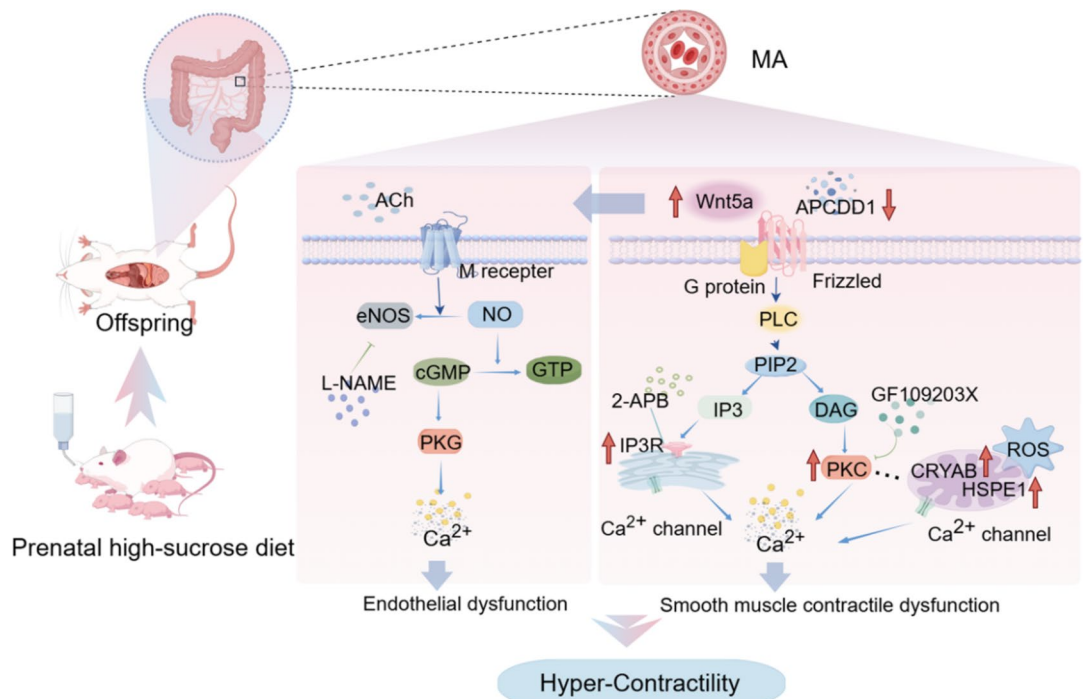


Fig. 7. Summarized image of vascular hyper-contraction in MAs from offspring exposure to prenatal HS. Prenatal HS mediated vascular hyper-contraction by regulating Wnt5a/Ca²⁺ signaling, as indicated by RNA-Seq. In vascular smooth muscle, Wnt5a could increase cytoplasmic Ca²⁺ levels by regulating PKC/IP3R functions. In addition, endothelial NO system dysfunction further contributed to vascular hyper-contraction in the offspring exposed to prenatal HS.

Data availability

The datasets generated and/or analyzed during the current study are available in the GEO repository (Accession Number GSE290103).

Received: 16 December 2024; Accepted: 6 March 2025

Published online: 17 March 2025

References

- Goran, M. I., Plows, J. F. & Ventura, E. E. Effects of consuming sugars and alternative sweeteners during pregnancy on aternal and child health: evidence for a secondhand sugar effect. *Proc. Nutr. Soc.* **78**, 262–271 (2019).
- Avena, N. M., Rada, P. & Hoebel, B. G. Evidence for sugar addiction: behavioral and neurochemical effects of intermittent, excessive sugar intake. *Neurosci. Biobehav. Rev.* **32**, 20–39 (2008).
- Marshall, N. E. et al. The importance of nutrition in pregnancy and lactation: lifelong consequences. *Am. J. Obstet. Gynecol.* **226**, 607–632 (2022).
- Foulquier, S. et al. Wnt signaling in cardiac and vascular disease. *Pharmacol. Rev.* **70**, 68–141 (2018).
- Willert, K. et al. Wnt proteins are Lipid-Modified and can act as stem cell growth factors. *Nature* **423**, 448–452 (2003).
- Tufail, M. & Wu, C. Wnt5a: A Double-Edged sword in colorectal Cancer progression. *Mutat. Res. -Rev. Mutat. Res.* **792**, 108465 (2023).
- Feng, X. et al. Activation of lysosomal Ca²⁺ Channels mitigates mitochondrial damage and oxidative stress. *J. Cell. Biol.* **224**, e202403104 (2025).
- Frismantiene, A., Philippova, M., Erne, P. & Resink, T. J. Smooth muscle Cell-Driven vascular diseases and molecular mechanisms of Vsmc plasticity. *Cell. Signal.* **52**, 48–64 (2018).
- Ghezzi, A. C. et al. Metabolic syndrome markers in Wistar rats of different ages. *Diabetol. Metab. Syndr.* **4**, 16 (2012).
- van Bezooijen, C. F. Influence of age-related changes in rodent liver morphology and physiology on drug metabolism—a review. *Mech. Ageing Dev.* **25**, 1–22 (1984).
- Kanehisa, M., Goto, S. & Kegg Kyoto encyclopedia of genes and genomes. *Nucleic Acids Res.* **28**, 27–30 (2000).
- Kanehisa, M. Toward Understanding the origin and evolution of cellular organisms. *Protein Sci.* **28**, 1947–1951 (2019).
- Kanehisa, M., Furumichi, M., Sato, Y., Kawashima, M. & Ishiguro-Watanabe, M. Kegg for Taxonomy-Based analysis of pathways and genomes. *Nucleic Acids Res.* **51**, D587–D592 (2023).
- Chen, L. J., Wei, S. Y. & Chiu, J. J. Mechanical regulation of epigenetics in vascular biology and pathobiology. *J. Cell. Mol. Med.* **17**, 437–448 (2013).
- Feng, X. et al. Prenatal High-Sucrose diet induced vascular dysfunction of renal interlobararteries in the offspring via Ppargamma-Rxrg-Ros/Akt signaling. *Mol. Nutr. Food Res.* **68**, e2300871 (2024).
- Stenmark, K. R., Frid, M. G., Graham, B. B. & Tuder, R. M. Dynamic and diverse changes in the functional properties of vascular smooth muscle cells in pulmonary hypertension. *Cardiovasc. Res.* **114**, 551–564 (2018).
- Marziano, C., Genet, G. & Hirschi, K. K. Vascular endothelial cell specification in health and disease. *Angiogenesis* **24**, 213–236 (2021).

18. Xu, L. et al. Ip3R2 regulates apoptosis by Ca²⁺ Transfer through Mitochondria-Er contacts in hypoxic photoreceptor injury. *Exp. Eye Res.* **245**, 109965 (2024).
19. Costa, T. J. et al. The homeostatic role of hydrogen peroxide, superoxide anion and nitric oxide in the vasculature. *Free Radic Biol. Med.* **162**, 615–635 (2021).
20. Li, X. et al. Prenatal hypoxia plus postnatal High-Fat diet exacerbated vascular dysfunction via Up-Regulated vascular Cav1.2 channels in offspring rats. *J. Cell. Mol. Med.* **23**, 1183–1196 (2019).
21. Rennison, J. H. & Van Wagoner, D. R. Dysregulated Ca²⁺ Cycling in atrial fibrillation. *Eur. Heart J.* **44**, 2495–2497 (2023).
22. Yang, D. H. et al. Wnt5a is required for endothelial differentiation of embryonic stem cells and vascularization via pathways involving both Wnt/Beta-Catenin and protein kinase Calpha. *Circ. Res.* **104**, 372–379 (2009).
23. Ye, X. et al. Frizzled-4, and Lrp5 signaling in endothelial cells controls a genetic program for retinal vascularization. *Cell* **139**, 285–298 (2009).
24. Sabadell-Basallote, J. et al. Sucnr1 regulates insulin secretion and glucose elevates the succinate response in people with prediabetes. *J. Clin. Invest.* **134**, e173214 (2024).
25. De, A. Wnt/Ca²⁺ Signaling pathway: A brief overview. *Acta Biochim. Biophys. Sin.* **43**, 745–756 (2011).
26. Tykocki, N. R., Boerman, E. M. & Jackson, W. F. Smooth muscle ion channels and regulation of vascular tone in resistance arteries and arterioles. *Compr. Physiol.* **7**, 485–581 (2017).
27. Kopincova, J., Puzserova, A. & Bernatova, I. L-Name in the cardiovascular System - Nitric oxide synthase activator?? *Pharmacol. Rep.* **64**, 511–520 (2012).

Acknowledgements

This work was supported by the National Natural Science Foundation of China (82101797), the Natural Science Foundation of Shandong Province (ZR2021QH131), Key Research and Development Program of Jining Science (2023YXNS030) and PhD Research Foundation of Affiliated Hospital of Jining Medical University (2021-BS-025). The authors would like to thank Shandong Jienuoxuan Biotechnology co.,ltd (Shandong, China) for whole-transcriptome sequencing and data analysis.

Author contributions

Xueqin Feng designed the experiments. Xinying Liu wrote the first draft, and Xueqin Feng revised the manuscript. Xueqin Feng and Dongmei Man had the primary responsibility for final content. Xinying Liu, Meng Liu, Hongwei Fu and Xiao Sun accomplished the measurement of vascular tension. Xinying Liu, Meng Liu and Chunxia Wang did the molecular detection. Liting Duan, Shuli Jiang, Jing Han and Qinggui Ren made a substantial contribution to animal feeding or sample preparation. All authors reviewed the manuscript.

Declarations

Competing interests

The authors declare no competing interests.

Additional information

Supplementary Information The online version contains supplementary material available at <https://doi.org/10.1038/s41598-025-93361-2>.

Correspondence and requests for materials should be addressed to D.M. or X.F.

Reprints and permissions information is available at www.nature.com/reprints.

Publisher's note Springer Nature remains neutral with regard to jurisdictional claims in published maps and institutional affiliations.

Open Access This article is licensed under a Creative Commons Attribution-NonCommercial-NoDerivatives 4.0 International License, which permits any non-commercial use, sharing, distribution and reproduction in any medium or format, as long as you give appropriate credit to the original author(s) and the source, provide a link to the Creative Commons licence, and indicate if you modified the licensed material. You do not have permission under this licence to share adapted material derived from this article or parts of it. The images or other third party material in this article are included in the article's Creative Commons licence, unless indicated otherwise in a credit line to the material. If material is not included in the article's Creative Commons licence and your intended use is not permitted by statutory regulation or exceeds the permitted use, you will need to obtain permission directly from the copyright holder. To view a copy of this licence, visit <http://creativecommons.org/licenses/by-nc-nd/4.0/>.

© The Author(s) 2025